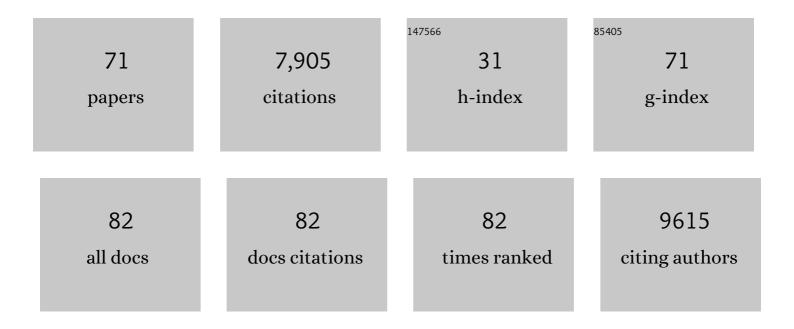
## **Stefan Stoll**

List of Publications by Year in descending order

Source: https://exaly.com/author-pdf/9219118/publications.pdf Version: 2024-02-01



STEEAN STOLL

#	Article	IF	CITATIONS
1	Dipolar pathways in dipolar EPR spectroscopy. Physical Chemistry Chemical Physics, 2022, 24, 2504-2520.	1.3	7
2	Compactness regularization in the analysis of dipolar EPR spectroscopy data. Journal of Magnetic Resonance, 2022, 339, 107218.	1.2	9
3	Mechanism of Electron Spin Decoherence in a Partially Deuterated Glassy Matrix. Journal of Physical Chemistry Letters, 2022, 13, 5474-5479.	2.1	8
4	The effect of spin polarization on double electron–electron resonance (DEER) spectroscopy. Magnetic Resonance, 2022, 3, 101-110.	0.8	5
5	Spectroscopic Investigation of a Metal–Metal-Bonded Fe <sub>6</sub> Single-Molecule Magnet with an Isolated <i>S</i> = <sup>19</sup> / <sub>2</sub> Giant-Spin Ground State. Inorganic Chemistry, 2021, 60, 4610-4622.	1.9	13
6	The decay of the refocused Hahn echo in double electron–electron resonance (DEER) experiments. Magnetic Resonance, 2021, 2, 161-173.	0.8	11
7	Determining electron–nucleus distances and Fermi contact couplings from ENDOR spectra. Physical Chemistry Chemical Physics, 2021, 23, 8326-8335.	1.3	5
8	Benchmark Test and Guidelines for DEER/PELDOR Experiments on Nitroxide-Labeled Biomolecules. Journal of the American Chemical Society, 2021, 143, 17875-17890.	6.6	124
9	Bayesian Probabilistic Analysis of DEER Spectroscopy Data Using Parametric Distance Distribution Models. Journal of Physical Chemistry A, 2020, 124, 6193-6202.	1.1	20
10	Modeling of motional EPR spectra using hindered Brownian rotational diffusion and the stochastic Liouville equation. Journal of Chemical Physics, 2020, 152, 094103.	1.2	13
11	Allosteric conformational change of a cyclic nucleotide-gated ion channel revealed by DEER spectroscopy. Proceedings of the National Academy of Sciences of the United States of America, 2020, 117, 10839-10847.	3.3	38
12	Exploiting chemistry and molecular systems for quantum information science. Nature Reviews Chemistry, 2020, 4, 490-504.	13.8	247
13	FBXL5 Regulates IRP2 Stability in Iron Homeostasis via an Oxygen-Responsive [2Fe2S] Cluster. Molecular Cell, 2020, 78, 31-41.e5.	4.5	87
14	Quantitative Structure-Based Prediction of Electron Spin Decoherence in Organic Radicals. Journal of Physical Chemistry Letters, 2020, 11, 3396-3400.	2.1	45
15	DeerLab: a comprehensive software package for analyzing dipolar electron paramagnetic resonance spectroscopy data. Magnetic Resonance, 2020, 1, 209-224.	0.8	93
16	Trajectory-Based Simulation of EPR Spectra: Models of Rotational Motion for Spin Labels on Proteins. Journal of Physical Chemistry B, 2019, 123, 10131-10141.	1.2	14
17	How Metal Ion Lewis Acidity and Steric Properties Influence the Barrier to Dioxygen Binding, Peroxo O–O Bond Cleavage, and Reactivity. Journal of the American Chemical Society, 2019, 141, 15046-15057.	6.6	15
18	Vanadyl Porphyrin Speciation Based on Submegahertz Ligand Proton Hyperfine Couplings. Energy & Fuels, 2019, 33, 4237-4243.	2.5	19

STEFAN STOLL

#	Article	IF	CITATIONS
19	Optimal Tikhonov regularization for DEER spectroscopy. Journal of Magnetic Resonance, 2018, 288, 58-68.	1.2	63
20	Photochemical changes in absorption and fluorescence of DDM-containing epoxies. Polymer, 2018, 142, 11-22.	1.8	8
21	Mechanochemical changes in absorption and fluorescence of DDM-containing epoxies. Polymer, 2018, 142, 132-143.	1.8	11
22	Determination of Large Zero-Field Splitting in High-Spin Co(I) Clathrochelates. Inorganic Chemistry, 2018, 57, 15330-15340.	1.9	12
23	ENDOR with band-selective shaped inversion pulses. Journal of Magnetic Resonance, 2017, 277, 36-44.	1.2	13
24	Rates and equilibrium constants of the ligand-induced conformational transition of an HCN ion channel protein domain determined by DEER spectroscopy. Physical Chemistry Chemical Physics, 2017, 19, 15324-15334.	1.3	32
25	Mechanism for the inhibition of the cAMP dependence of HCN ion channels by the auxiliary subunit TRIP8b. Journal of Biological Chemistry, 2017, 292, 17794-17803.	1.6	23
26	EPR Study of UV-Irradiated Thymidine Microcrystals Supports Radical Intermediates in Spore Photoproduct Formation. Journal of Physical Chemistry B, 2016, 120, 10923-10931.	1.2	3
27	A Bayesian approach to quantifying uncertainty from experimental noise in DEER spectroscopy. Journal of Magnetic Resonance, 2016, 270, 87-97.	1.2	66
28	Coherent pump pulses in Double Electron Electron Resonance spectroscopy. Physical Chemistry Chemical Physics, 2016, 18, 18470-18485.	1.3	57
29	Electronic Structure of a Cu <sup>II</sup> –Alkoxide Complex Modeling Intermediates in Copper-Catalyzed Alcohol Oxidations. Journal of the American Chemical Society, 2016, 138, 4132-4145.	6.6	12
30	Structure and Energetics of Allosteric Regulation of HCN2 Ion Channels by Cyclic Nucleotides. Journal of Biological Chemistry, 2016, 291, 371-381.	1.6	41
31	General Magnetic Transition Dipole Moments for Electron Paramagnetic Resonance. Physical Review Letters, 2015, 114, 010801.	2.9	27
32	Structural Mechanism for the Regulation of HCN Ion Channels by the Accessory Protein TRIP8b. Structure, 2015, 23, 734-744.	1.6	36
33	Simulating Frequency-Domain Electron Paramagnetic Resonance: Bridging the Gap between Experiment and Magnetic Parameters for High-Spin Transition-Metal Ion Complexes. Journal of Physical Chemistry B, 2015, 119, 13816-13824.	1.2	47
34	Conformational Change with Steric Interactions Affects the Inner Sphere Component of Concerted Proton–Electron Transfer in a Pyridyl-Appended Radical Cation System. Journal of Organic Chemistry, 2015, 80, 8705-8712.	1.7	3
35	CW-EPR Spectral Simulations. Methods in Enzymology, 2015, 563, 121-142.	0.4	25
36	Oxygenâ€Promoted CH Bond Activation at Palladium. Angewandte Chemie - International Edition, 2014, 53, 6492-6495.	7.2	26

STEFAN STOLL

#	Article	IF	CITATIONS
37	Double electron–electron resonance reveals cAMP-induced conformational change in HCN channels. Proceedings of the National Academy of Sciences of the United States of America, 2014, 111, 9816-9821.	3.3	85
38	Double Electron-Electron Resonance Studies of Ligand Induced Rearrangements of HCN Channels. Biophysical Journal, 2014, 106, 737a.	0.2	0
39	Zero-field splittings in metHb and metMb with aquo and fluoro ligands: a FD-FT THz-EPR study. Molecular Physics, 2013, 111, 2696-2707.	0.8	36
40	Spectroscopic Investigation of Agonist-Induced Rearrangements of Cyclic Nucleotide-Modulated Ion Channels. Biophysical Journal, 2013, 104, 271a.	0.2	0
41	Formation of MgO-Supported Manganese Carbonyl Complexes by Chemisorption of Mn(CO) <sub>5</sub> CH <sub>3</sub> . Langmuir, 2013, 29, 6279-6286.	1.6	9
42	Monotrimethylene-Bridged Bis- <i>p</i> -phenylenediamine Radical Cations and Dications: Spin States, Conformations, and Dynamics. Journal of Physical Chemistry A, 2013, 117, 1439-1448.	1.1	15
43	A Radical Transfer Pathway in Spore Photoproduct Lyase. Biochemistry, 2013, 52, 3041-3050.	1.2	32
44	Double electron–electron resonance shows cytochrome P450cam undergoes a conformational change in solution upon binding substrate. Proceedings of the National Academy of Sciences of the United States of America, 2012, 109, 12888-12893.	3.3	50
45	Reduction of the [2Fe–2S] Cluster Accompanies Formation of the Intermediate 9-Mercaptodethiobiotin in <i>Escherichia coli</i> Biotin Synthase. Biochemistry, 2011, 50, 7953-7963.	1.2	34
46	A Redox Series of Aluminum Complexes: Characterization of Four Oxidation States Including a Ligand Biradical State Stabilized via Exchange Coupling. Journal of the American Chemical Society, 2011, 133, 8662-8672.	6.6	95
47	Hydrogen Bonding of Tryptophan Radicals Revealed by EPR at 700 GHz. Journal of the American Chemical Society, 2011, 133, 18098-18101.	6.6	52
48	Atomic hydrogen as high-precision field standard for high-field EPR. Journal of Magnetic Resonance, 2010, 207, 158-163.	1.2	34
49	Binding of Histidine in the (Cys) <sub>3</sub> (His) <sub>1</sub> -Coordinated [2Feâ^'2S] Cluster of Human mitoNEET. Journal of the American Chemical Society, 2010, 132, 2037-2049.	6.6	67
50	Structural Basis for Hydration Dynamics in Radical Stabilization of Bilin Reductase Mutants. Biochemistry, 2010, 49, 6206-6218.	1.2	15
51	Formation of a Manganese Tricarbonyl on the MgO Surface from Mn <sub>2</sub> (CO) <sub>10</sub> : Characterization by Infrared, Electron Paramagnetic Resonance, and X-ray Absorption Spectroscopies. Journal of Physical Chemistry C, 2010, 114, 17212-17221.	1.5	5
52	Nitric Oxide Synthase Stabilizes the Tetrahydrobiopterin Cofactor Radical by Controlling Its Protonation State. Journal of the American Chemical Society, 2010, 132, 11812-11823.	6.6	78
53	Interaction of PqqE and PqqD in the pyrroloquinoline quinone (PQQ) biosynthetic pathway links PqqD to the radical SAM superfamily. Chemical Communications, 2010, 46, 7031.	2.2	43
54	NO formation by a catalytically self-sufficient bacterial nitric oxide synthase from <i>Sorangium cellulosum</i> . Proceedings of the National Academy of Sciences of the United States of America, 2009, 106, 16221-16226.	3.3	59

STEFAN STOLL

#	Article	IF	CITATIONS
55	Structure of the Biliverdin Radical Intermediate in Phycocyanobilin:Ferredoxin Oxidoreductase Identified by High-Field EPR and DFT. Journal of the American Chemical Society, 2009, 131, 1986-1995.	6.6	38
56	General and efficient simulation of pulse EPR spectra. Physical Chemistry Chemical Physics, 2009, 11, 6614.	1.3	136
57	Pyrroloquinoline Quinone Biogenesis: Demonstration That PqqE from <i>Klebsiella pneumoniae</i> Is a Radical <i>S</i> -Adenosyl- <scp>l</scp> -methionine Enzyme. Biochemistry, 2009, 48, 10151-10161.	1.2	84
58	Nuclear relaxation effects in Davies ENDOR variants. Journal of Magnetic Resonance, 2008, 191, 315-321.	1.2	12
59	Phase Cycling in Electron Spin Echo Envelope Modulation. Applied Magnetic Resonance, 2008, 35, 15-32.	0.6	17
60	5- and 6-pulse electron spin echo envelope modulation (ESEEM) of multi-nuclear spin systems. Journal of Magnetic Resonance, 2008, 190, 233-247.	1.2	28
61	Ligand protons in a frozen solution of copper histidine relax via a T1e-driven three-spin mechanism. Journal of Chemical Physics, 2007, 127, 164511.	1.2	20
62	Raman intensity mapping of single-walled carbon nanotubes. Physical Review B, 2007, 75, .	1.1	23
63	Matrix effects on copper(ii)phthalocyanine complexes. A combined continuous wave and pulse EPR and DFT study. Physical Chemistry Chemical Physics, 2006, 8, 1942.	1.3	51
64	EasySpin, a comprehensive software package for spectral simulation and analysis in EPR. Journal of Magnetic Resonance, 2006, 178, 42-55.	1.2	5,100
65	Pulse EPR Methods for Studying Chemical and Biological Samples Containing Transition Metals. Helvetica Chimica Acta, 2006, 89, 2495-2521.	1.0	44
66	Peak suppression in ESEEM spectra of multinuclear spin systems. Journal of Magnetic Resonance, 2005, 177, 93-101.	1.2	95
67	Spectrometer manager: A versatile control software for pulse EPR spectrometers. Concepts in Magnetic Resonance Part B, 2005, 26B, 36-45.	0.3	81
68	An adaptive method for computing resonance fields for continuous-wave EPR spectra. Chemical Physics Letters, 2003, 380, 464-470.	1.2	30
69	Rapid construction of solid-state magnetic resonance powder spectra from frequencies and amplitudes as applied to ESEEM. Journal of Magnetic Resonance, 2003, 163, 248-256.	1.2	13
70	Continuous wave and pulse EPR as a tool for the characterization of monocyclopentadienyl Ti(III) catalysts. Journal of Organometallic Chemistry, 2001, 634, 185-192.	0.8	18
71	Nutation-Frequency Correlated EPR Spectroscopy: The PEANUT Experiment. Journal of Magnetic Resonance, 1998, 130, 86-96.	1.2	68